International Journal of Theoretical & Applied Sciences, **5**(1): 1-8 (2013)
ISSN No. (Print): 0975-1718
ISSN No. (Online): 2249-3247

Cu_2ZnSnS_4 and $Cu_2ZnSnSe_4$ as Potential Earth-Abundant Thin-Film Absorber Materials: A Density Functional Theory Study

Mukesh Kumar* and Clas Persson**
**Department of Materials Science and Engineering, Royal Institute of Technology, SE–100 44 Stockholm, Sweden*
***Department of Physics, University of Oslo, P.O. Box 1048 Blindern, NO–0316 Oslo, Norway*

(Received 05 November, 2012, Accepted 02 December, 2012)

ABSTRACT: In this work we systematically analyze the structural, electronic and optical properties of the Cu_2ZnSnS_4 and $Cu_2ZnSnSe_4$. We show that kesterite is more stable phase than the stannite phase and the estimated direct band gaps energy for $Cu_2ZnSn(S, Se)_4$ compounds ranges from 0.70 to 1.47 eV. Furthermore, defect studies reveal that Cu vacancy is the most dominant vacancy with the lowest formation energy. We find that the vacancy formation energies are larger in the Cu_2ZnSnS_4 compared with the corresponding vacancies in the $Cu_2ZnSnSe_4$. All the calculations are carried out by employing hybrid functional approach within the density functional theory.

Keywords: $Cu_2ZnSn(S, Se)_4$; solar cells; electronic structure, defect formation energy; density functional theory.

I. INTRODUCTION

Development of photovoltaic materials (PV) comprised of non-toxic, earth abundant elements are considered to be a major criterion to meet the ever increasing demand for energy [1]. Current PV technologies are mostly dominated by the two most promising thin-films solar cells *i.e.*, CdTe [2] and $Cu(In,Ga)Se_2$ (CIGS) [3]. However, due to price volatility issues (In, Ga), supply issues (In, Te), and environmental issues (Cd), these solar cell technologies are under scanner [4]. Hence, the current research efforts are directed to search the new inexpensive and earth abundant materials as thin-film solar cells. To meet the aforementioned demands, one of the suitable candidates is $Cu_2ZnSn(S,Se)_4$ (CZTSSe) type compound, primarily because they contain only the abundant and inexpensive elements like Cu, Zn, Sn, S, and Se in compared with the corresponding CIGS. Apart from this, the band gap energy of the CZTSSe ranges between E_g = 1.0–1.6 eV which fall in the optimum band gap range and they also have high absorption coefficient ($>10^4$ cm^{-1}) which is suitable for PV applications. Furthermore, a solar cell conversion efficiency of 11.1% [Nov. 2012] has already been achieved [5]. Therefore, more attention has been given to Cu_2ZnSnS_4 (CZTS) and $Cu_2ZnSnSe_4$ (CZTSe) in recent time [6-18]. For these materials, two types of crystal structures namely kesterite (ks) and stannite (st) have been reported both experimentally [14-18] and theoretically [19-21]. A theoretical method especially first-principles within density functional theory (DFT) is of special priority in the study of electronic and structural properties of materials due to its superiority in control. Since, the DFT using the local density approximation (LDA) or semilocal generalized gradient approximations (GGA) with the semilocal Perdew-Burke-Ernzerhof (PBE) [22] exchange-correlation functional are in general fails to reproduce band gaps and lattice parameters comparable with experiment findings, therefore, in this work we use a hybrid Heyd-Scuseria-Ernzerhof (HSE06) [23] functional to overcome these problems. The defect studies are performed using the supercell approach. The Crystal structure, density of states, band structure, optical properties, and formation energy (ΔH_f) of native neutral defects of CZTSSe are discussed in details. We show that, CZTS and CZTSe have comparable electronic and optical properties with band gap energy estimated to be E_g = 1.27–1.47 eV for CZTS and E_g = 0.70–0.90 eV for CZTSe. Total energy calculation reveals that kesterite is more stable phase than the stannite phase. Furthermore, defect studies revealed that Cu vacancy is the most dominant vacancy with the lowest formation energy ΔH_f. The formation energy of Cu vacancy is very similar in the both compounds. Moreover, we demonstrate that the vacancy formation energies are larger in the CZTS compared with the corresponding vacancies in the CZTSe.

II. COMPUTATIONAL DETAILS

All the calculations are performed using the DFT method as implemented in Vienna *ab initio* simulation package [24]. Wave functions are represented by plane-wave basis with projector augmented wave (PAW) method [25]. For the intrinsic compounds, a plane wave cutoff energy of 450 eV and a 8 × 8 × 4 Monkhorst-Pack **k**-point mesh are used to give converged results. For defect studies, we construct the defects in a 64-atoms super cell and estimated the defect formation energy by using a plane wave cutoff energy of 350 eV and a **k**-point mesh of 4×4×4 size. For HSE06 calculation, a 25% screened Hartree-Fock exchange with a standard Hartree-Fock screening parameter 0.2 is choose which is known to fairly accurately describe the crystal volume and band gap energies. The ion positions of the calculated cell are fully relaxed with the maximum force on each atom below 0.01 eV/Å, whereas the lattice constants are relaxed by minimizing the total energy to an accuracy of 0.1 meV. The valance electrons include the 3*d* and 4*s* orbitals for Cu and Zn and open-shell *s* and *p* orbitals for Sn, In, S, and Se.

III. RESULTS AND DISCUSSION

A. Crystal structure

Fig. 1 shows the crystal structure of CZTSSe and CISSe compounds. For the ks-structure (Fig 1a) [$I\bar{4}$; space group no. 82], four Cu atoms are on the Wyckoff positions 2*a* and 2*c*, two Zn atoms on position 2*d*, two Sn atoms on position 2*b*, and eight anions (S or Se) atoms on the 8*g* position, while for st-structure (Fig. 1b) [$I\bar{4}2m$; space group no. 121], the four equivalent Cu atoms on the Wyckoff 4*d* positions, two Zn atoms on position 2*a*, two Sn atoms on position 2*b*, and eight anions (S or Se) atoms on the 8*i* position. Similarly, for the chalcopyrite CISSe compounds, we used most stable tetragonal structure (fig. 1c) [$I\bar{4}2d$; space group no. 122] and perform a comparative study together with CZTSSe in order to understand these chalcogenide compounds better. Table 1 shows the calculated lattice parameters (*a*, and *c*), anion position (*x*, *y*, *z*), total energy difference (ΔE_t) band gap energy (E_g), and high frequency dielectric constants (ε_∞) calculated with HSE06. The calculated values of CZTSSe and CISSe are in satisfactory agreement with experimental as well the available theoretical data. These results demonstrate that the HSE functional improves the reproduction of lattice parameters and band gap energy with the experimental values. From the calculated total energy difference $\Delta E_t = E_t(\text{st}) - E_t(\text{ks})$ the most stable phase is the ks-structure and this is agree well with the recent experimental results. However, other phase stannite can also be grown as the lattice parameters, total energy, and bond lengths are almost similar for both the phases (Table 1).

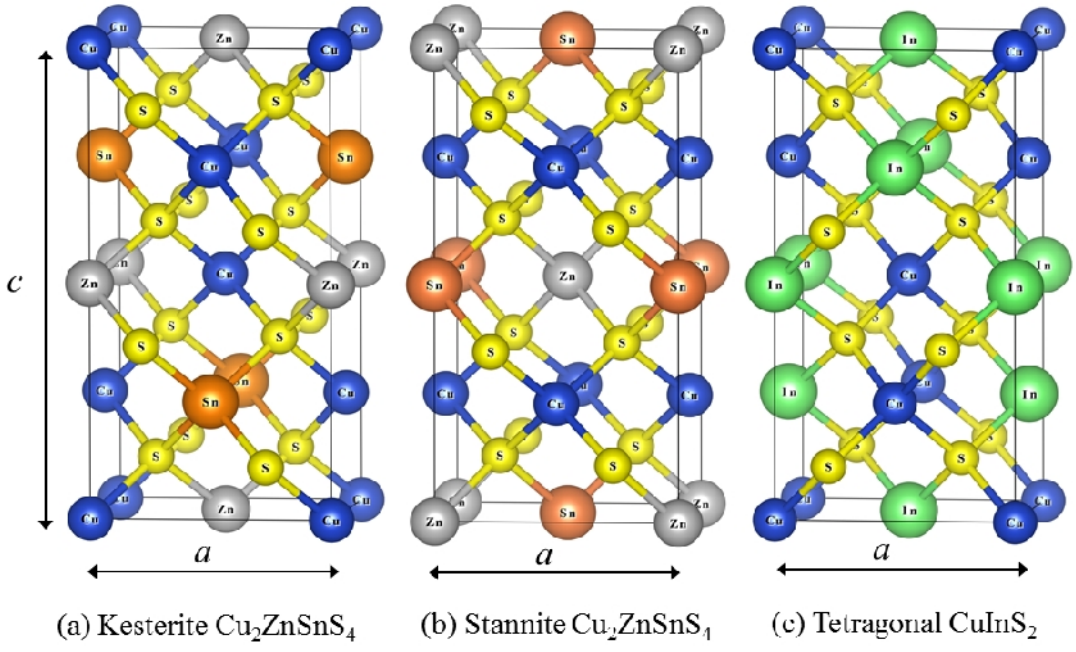

Fig. 1. Crystal structure of (a) kesterite-CZTS, (b) stannite-CZTS, and (c) tetragonal-CIS.

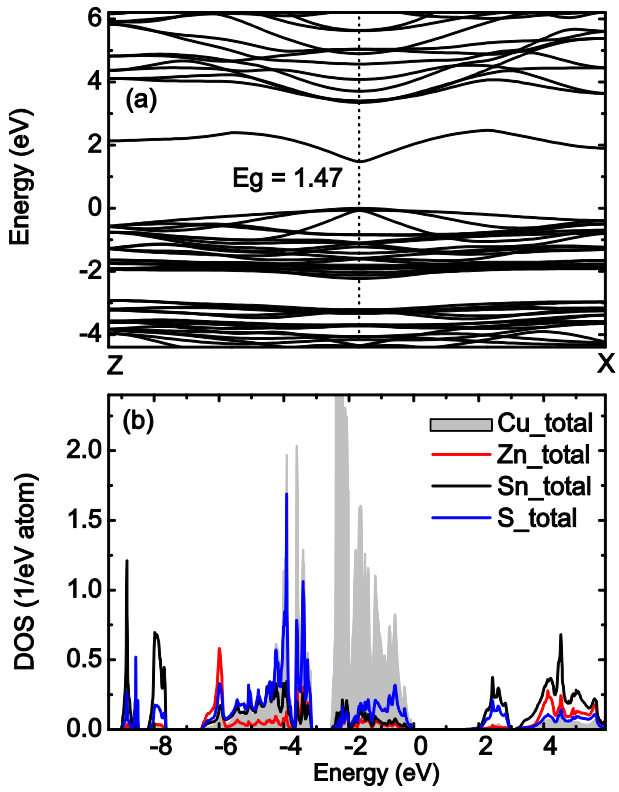

Fig. 2. (a) Calculated electronic band structure along two symmetry lines Z (001-direction) and X (110-direction) for ks-CZTS as a representative case. All the compounds show rather similar band structure with a fundamental direct bad gap at Γ-point. The energies are referred to the VBM (dashed line). (b) Atomic - resolved DOS of ks-CZTS. The grey area represents the DOS of Cu atom, while red, black and blue lines represent the DOS of Zn, Sn, and S atoms respectively.

Table 1. Calculated lattice constants (*a* and *c*), bond lengths between the cation (Cu, In, Zn, or Sn) and the anion (S or Se), the difference in total energy per primitive cell ΔE_t, band gap energies E_g, and high-frequency dielectric constants ε_∞ of the kesterite, stannite, and chalcopyrite structured CZTSSe and CISSe compound with the HSE06 exchange-correlation potentials.

	Cu_2ZnSnS_4		$Cu_2ZnSnSe_4$		$CuInS_2$	$CuInSe_2$
	Kesterite	Stannite	Kesterite	Stannite	Tetragonal	
a (Å)	5.440	5.450	5.732	5.738	5.555	5.829
c (Å)	10.864	10.878	11.418	11.453	11.187	11.700
$\delta_{Cu(1)-Y}$ (Å)	2.33	2.32	2.44	2.439	2.33	2.45
$\delta_{Cu(2)-Y}$ (Å)	2.33	2.33	2.45	2.438		
δ_{Zn-Y} (Å)	2.35	2.36	2.47	2.49		
δ_{Sn-Y} (Å)	2.42	2.42	2.56	2.57		
δ_{In-Y} (Å)					2.54	2.64
ΔE_t (meV/cell)	0	50	0	64		
E_g (eV)	1.47 (1.50[a])	1.27(1.38[a])	0.90 (0.96[a])	0.70(0.82[a])	1.25 (1.33[b])	0.79 (0.85[b])
ε_∞	6.31	6.36	7.58	8.05	6.17	7.81

[a]Reference 19, [b]Reference 21

B. Electronic properties

(i) Full-band structure

Fig. 2a shows the electronic band structure of ks-Cu_2ZnSnS_4 as a representative case (we show only CZTS compound, because all these compounds have rather similar band structures and chemical bonding environment). One can see that CZTS as well others have a direct band gap as valence band maxima (VBM) and conduction band minima (CBM) is located at Γ-point. The estimated HSE06 band gap energy is E_g= 1.47 eV for ks-CZTS, 1.27 eV for st-CZTS, 0.90 eV for ks-CZTSe and 0.70 eV for st-CZTSe. It demonstrates that the theoretical band gap of CZTSe is about 0.57 eV smaller than that of CZTS, which is agree well with an energy difference of $\Delta E_g \approx 0.5$ eV [14]. Very early measurements [15] indicated that E_g(CZTSe) = 1.44 eV, which disagrees with our calculated band gap, and the reason for this could be (as reported by Chen *et al.* [19]) either poor sample quality or incorrect linear interpolation of the gap energies. Moreover, our calculated band gap energies are in good agreement with earlier theoretical predictions [19,21]. Similarly for CISSe compounds our calculated HSE06 band gap energies, E_g = 1.25 eV for $CuInS_2$ and E_g = 0.79 eV for $CuInSe_2$ are in good agreement with earlier experimental [26] and theoretical [27] findings (Table 1).

(ii) Density of States

In order to analyze the chemical bonding, Fig 2b shows the Atomic - resolved density of states (DOS) of ks-CZTS as a representative case. The valance band (VB) DOS contains mainly a hybridization of Cu-3*d* and anion *p*(S, Se), similar to other Cu-S based semiconductor CIGS [20]. The contribution of Zn-*spd*, Cu-*s*, and Sn-*p* can also be seen in the lower energy region from -6 to -2 eV of the DOS. One can also see the peaks of anion (S, Se) *s* and *p* states well below the VBM at –10 to –8 eV and –10 to –8 eV, respectively. On the other hand top of the conduction band (CB) consists mainly of a Sn-*s* and anion-*p* (S, Se) hybridization. One can also see that the difference between the lowest CB and next higher lying CBs is about 2 eV and such higher CBs do not contributes to the optical absorption in the low energy regime [20].

C. Optical properties

In this section, the optical properties are presented in terms of the complex dielectric function $\varepsilon_1(\omega) + i\varepsilon_2(\omega)$ and absorption coefficient $\alpha(\omega)$.

(i) Dielectric functions

One of the main optical characteristics of a solid is its complex dielectric function. The imaginary part ε_2 of the dielectric function is calculated from the joint DOS integrated over the Brillouin zone with the weight of momentum matrix elements while real part ε_1 is related to the imaginary part by Kramers-Kronig transformation [20]. Fig. 3 shows the dielectric function $\varepsilon(\omega)$ of CZTSSe compounds. All four compounds have similar dielectric function and the spectra are also comparable to CISSe (Fig. 3d). It is obvious form Fig. 3 that the dielectric functions show a significant anisotropy of its components perpendicular and parallel to the *c*-axis. The average high frequency dielectric constants ε_∞ calculated with HSE06 are shown in table 1. The ε_2 is dominated by a broad peak that extends between an absorption edge at 2.0–2.5 eV. St-compounds show much stronger anisotropy both in real and imaginary parts. The Se based compounds show larger high frequency dielectric constants (Table 1) and this is obvious as Se based compounds have low band gaps than S based compounds.

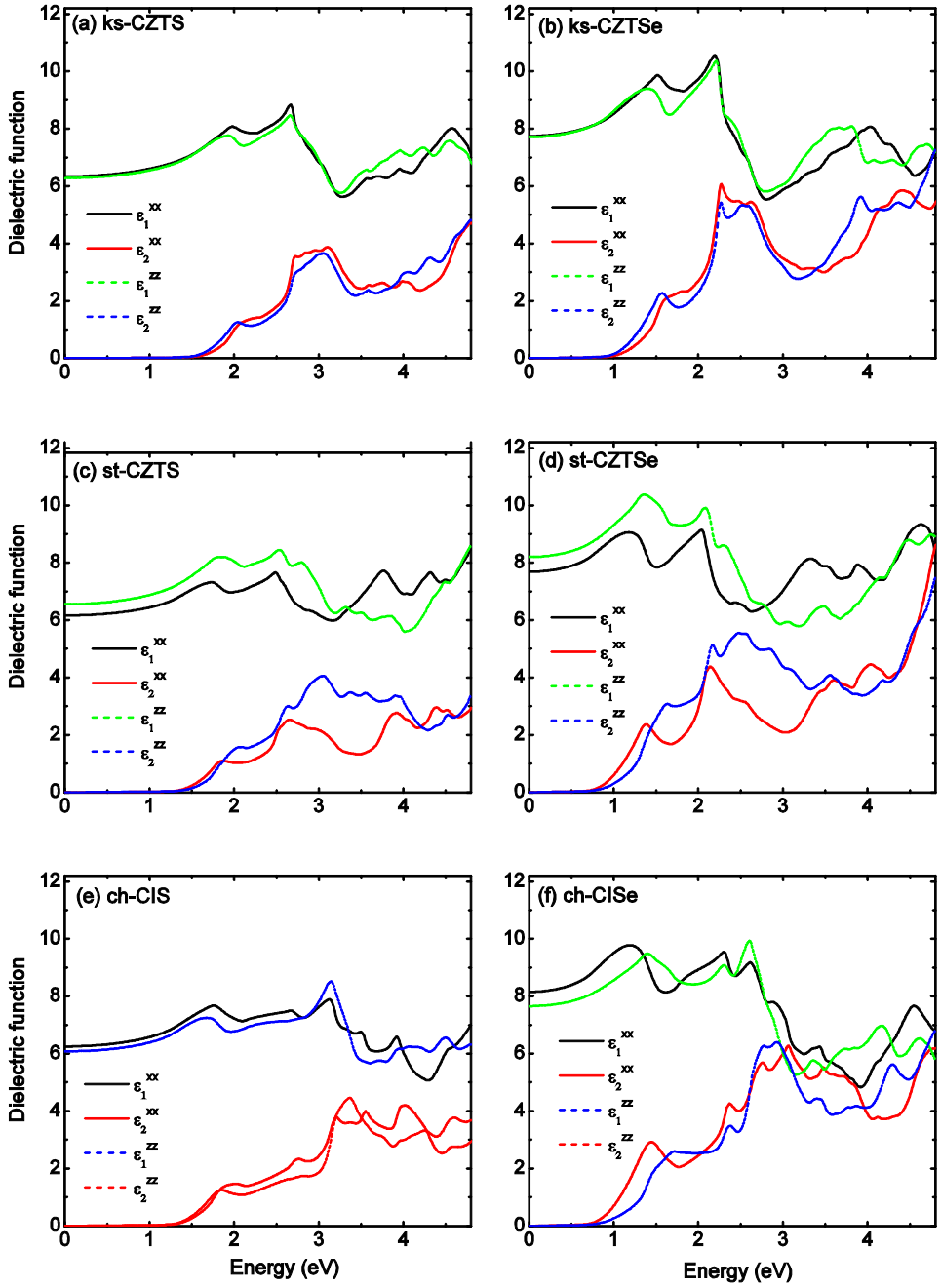

Fig. 3. The dielectric function $\varepsilon(\omega) = \varepsilon_1(\omega) + i\varepsilon_2(\omega)$ for (a) ks-CZTS, (b) ks- CZTSe, (c) St-CZTS, (d) st-CZTSe, (e) ch-CIS, and (f) ch-CISe calculated from HSE06. Here, the thin black and green lines represent the real part $\varepsilon_1(\omega)$, while red and blue lines represents the imaginary part $\varepsilon_2(\omega)$. Both the transverse (*xy*; solid lines) and longitudinal (*z*; dotted lines) are shown.

(ii) Absorption coefficient

The absorption coefficient $\alpha(\omega)$ is obtained directly from the dielectric function by

$$\alpha(\omega) = \frac{\sqrt{2\omega}}{c}\left[\sqrt{\varepsilon_1(\omega)^2 + \varepsilon_2(\omega)^2} - \varepsilon_1(\omega)\right]^{1/2}$$ where c is the speed of light. The calculated absorption coefficients of CZTSSe compounds are displayed in Fig. 4.

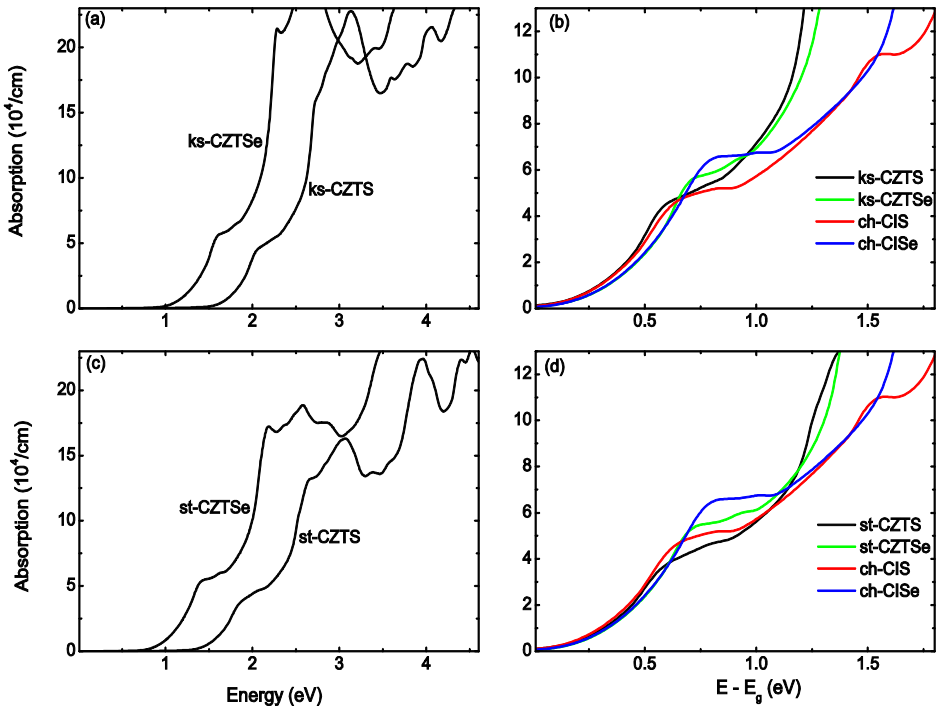

Fig.4. The absorption coefficient $\alpha(\omega)$ for the selected compounds. Left panel shows the absorption coefficient of (a) kesterite and (c) stannite structured CZTS and CZTSe compounds. Right panel shows the comparative behavior of (b) kesterite and, (d) stannite structured CZTSSe with chalcopyrite structured CISSe compounds.

For a comparison, we also show for CISSe compounds. Since the absorption is obtained directly from the dielectric function, similarities in the polarization response are reflected also in the absorption coefficient. Thus, all four compounds have comparable absorption except onset to absorption. One can see that ks-CZTS have much stronger absorption than the CZTSe and CISSe and which is as per experimental measurements. Overall, all these compounds have a much stronger absorption ($>10^4$ cm^{-1}) which is a desirable characteristic of the potential absorber materials for solar cell applications. Absorption measurement reveals the optical band gap of E_g= 1.51 eV for ks-CZTS, 1.38 eV for st-CZTS, 1.0 eV for ks-CZTSe, and 0.85 eV for st-CZTSe.

D. Defect studies

We perform the defect calculations of cation and anion vacancies using the supercell approach. The defect formation energy ΔH_f of neutral vacancies V_α is calculated following the procedure proposed in Refs 28 and 29:

$$\Delta H_f(V_\alpha, q = 0) = \Delta E(V_\alpha, q = 0) + \sum_\alpha n_\alpha \mu_\alpha , \quad ...(1)$$

where

$$\Delta E(V_\alpha, q = 0) = E_{tot}(V_\alpha, q = 0) - E_{tot}(0) \quad ...(2)$$

for

α = Cu, Zn, Sn, In, S or Se.

Here, $E_{tot}(V_\alpha, q = 0)$ represent the total energy of a supercell containing the neutral (q = 0) vacancy, and $E_{tot}(0)$ is the total energy of the defect free material. n_α is the number of atoms (Cu, Zn, Sn, In, S or Se) that are removed from the supercell when forming the structures with vacancies. These atoms are regarded to be in a reservoir with an absolute value of the chemical potential described by $\mu_\alpha = \mu_\alpha^{solid} + \Delta\mu_\alpha$, where the reference chemical potential μ_α^{solid} is the total energy of the ground state solid atoms like fcc structured Cu, hcp structured Zn, tetragonal structured Sn and In, and hexagonal structured S and Se. We restricted the chemical potential difference $\Delta\mu_\alpha = 0$ for each vacancy calculation, which mean that the formation energy of each vacancy is calculated in respective rich conditions. Table 3 comprises the calculated formation energies of neutral cation and anion vacancies of the CZTSSe (ks-structure only, as it is found to be the most stable phase) and CISSe compounds.

The calculated formation energy of V_{Cu}= 0.75 eV in CZTS with PBE is in good agreement with the value of 0.77 eV calculated by Chen and co-workers [30] using the same approximation. We found the formation energy of the Cu vacancy is lower than those energies of Zn and Sn vacancies. Sn vacancy has highest energy of formation. Similar to CZTSSe, also in the CISSe compounds the formation energy of V_{Cu} is very low, thus, V_{Cu} is a dominant native defect in both CZTSSe and CISSe. This is in agreement with the well-established fact that V_{Cu} is the main *p*-type acceptor in CIGS materials [28]. From Table 2 one can observe that the formation energy of V_{Cu} is almost similar in both *i.e.* same anion based corresponding compounds. However, an interesting trend is observed in case of V_{In}. The formation energy of V_{In} is roughly the average of formation energies of V_{Zn} and V_{Sn} [29]. Overall, we found that formation energy of V_{Cu} in Cu-rich condition is similar for one and the same anion based compound, that is, in Cu_2ZnSnS_4 and $CuInS_2$ or in $Cu_2ZnSnSe_4$ and $CuInSe_2$. Similar trends are observed also for neutral anion vacancies (V_S and V_{Se}), the formation energy of V_S are larger than that of V_{Se}.

Table 2. Calculated formation energy ΔH_f of neutral cation and anion vacancies of the CZTS, CZTSe, CIS and CISe compound by using the GGA and HSE06 potentials. The energies are in units of eV.

	PBE						HSE06
	V_{Cu}	V_{Zn}	V_{Sn}	V_{In}	V_S	V_{Se}	V_{Cu}
ks-CZTS	0.74 (0.77[a])	2.16	3.30		1.92		1.70
ks-CZTSe	0.46	1.74	2.67			1.65	1.37
CIS	0.75 (0.61[b])			2.76	2.07		1.74 (1.74[b])
CISe	0.44 (0.43[b])			2.32		1.88	1.38 (0.92[b])

[a]Reference 29, [b]Reference 27

IV. CONCLUSIONS

The structural, electronic, optical properties, and defect studies of Cu_2ZnSnS_4 and $Cu_2ZnSnSe_4$ have been analyzed theoretically. It has been found that these materials have rather similar electronic band structure and optical absorption coefficients. Total energy calculation reveals that kesterite phase is more stable than stannite phase. The calculated direct band gaps energy for $Cu_2ZnSn(S,Se)_4$ compounds ranges from 0.70 to 1.47 eV, which are in good agreement with previous measured values. The gaps are larger for the kesterite structured compared with the corresponding stannite structures. The gap energy of sulfur based compounds is more [E_g(ks-CZTS) = 1.47 eV] than corresponding to selenium based [E_g(ks-CZTSe) = 0. 90 eV] compounds. i.e. ΔEg = 0.57 eV, which is in good agreement with experimental finding. All these compounds have much large absorption coefficients ($>10^{-4}$ cm^{-1}), which is a desire characteristic for a good absorber material. CZTS show much larger absorption coefficient than CZTSe. From defect calculation, we reveal that the Cu vacancy is the most prominent neutral defect and it has very similar formation energy in both CZTSSe and CISSe compounds. The formation energies of cation vacancies are higher in the S based (CZTS) compounds compared with the corresponding Se based (CZTSe) compounds.

ACKNOWLEDGEMENTS

This work is supported by the Swedish Energy Agency, the Swedish Research Council, and the computers centers NSC and HPC2N through SNIC/SNAC and Matter network. M. K. and C. P. acknowledge the Swedish Institute and Erasmus Mundus External Cooperation Window program India4EU for financial support.

REFERENCES

[1]. C. Wadia, A. P. Alivisatos, and D.M. Kammen, *Environ. Sci. Technol*. **43**, 2072 (2009).

[2]. X. Wu, *Sol. Energy*, **77,** 803 (2004).

[3]. S. Siebentritt, M. Igalson, C. Persson, and S. Lany, *Prog. Photovolt: Res. Appl*. **18**, 390 (2010).

[4]. Critical Materials Strategy, U.S. Department of Energy, (2010).

[5]. T.K. Todorov, J. Tang, S. Bag, O. Gunawan, T. Gokmen, Y. Zhu, and D. B. Mitzi, *Adv. Mater.* **3**, 34 (2013).

[6]. K. Ito and T. Nakazawa, *Jpn. J. Appl. Phys. Part* 1, **27**, 2094 (1988).

[7]. H. Katagiri, N. Ishigaki, T. Ishida, and K. Saito, *Jpn. J. Appl. Phys. Part 1* **40**, 500 (2001).

[8]. K. Jimbo, R. Kimura, T. Kamimura, S. Yamada, W.S. Maw, H. Araki, K. Oishi, and H. Katagiri, *Thin Solid Films* **515**, 5997 (2007).

[9]. H. Katagiri, K. Jimbo, S. Yamada, T. Kamimura, W.S. Maw, T. Fukano, T. Ito, and T. Motohiro, *Appl. Phys. Express* **1**,041201 (2008).

[10]. A. Ennaoui, M. Lux-Steiner, A. Weber, D. Abou-Ras, I. Kötschau, H.-W.Schock, R. Schurr, A. Hölzing, S. Jost, R. Hock, T. Voß, J. Schulze, and A. Kirbs, *Thin Solid Films* **517**, 2511 (2009).

[11]. T.K. Todorov, K.B. Reuter, and D.B. Mitzi, *Adv. Mater.* **22**, E156 (2010).

[12]. H. Katagiri, K. Saitoh, T. Washio, H. Shinohara, T. Kurumadani, and S. Miyajima, *Sol. Energy Mater. Sol. Cells* **65**, 141 (2001).

[13]. R. Haight, A. Barkhouse, O. Gunawan, B. Shin, M. Copel, M. Hopstaken, and D. B. Mitzi, *Appl. Phys. Lett.* **98**, 253502 (2011).

[14]. J. He, L. Sun, S. Chen, Y. Chen, P. Yang, and J. Chu, *J. Alloys and Compd*. **511**, 129 (2012).

[15]. H. Matsushita, T. Maeda, A. Katsui, and T. Takizawa, *J. Cryst. Growth*, **208**, 416 (2000).

[16]. J.J. Scragg, P.J. Dale, and L.M. Peter, *Electrochem. Commun*., **10**, 639 (2008).

[17]. J.S. Seol, S.Y. Lee, J.C. Lee, H.D. Nam, and K.-H. Kim, *Sol. Energy Mater. Sol. Cells*, **75**, 155 (2003).

[18]. T. Tanaka, T. Nagatomo, D. Kawasaki, M. Nishio, Q. Guo, A. Wakahara, A. Yoshida, and H. Ogawa, *J. Phys. Chem. Solids*, **66**, 1978 (2005).

[19]. S. Chen, X. G. Gong, A. Walsh, and S. H. Wei, *Appl. Phys. Lett.* **94**, 041903 (2009).

[20]. C. Persson, *J. Appl. Phys*., **107**, 053710 (2010).

[21]. J. Paier, R. Asahi, A. Nagoya, and G. Kresse, *Phys. Rev.* ***B*** **79** 115126 (2009).

[22]. J.P. Perdew, J.A. Chevary, S.H. Vosko, K.A. Jackson, M.R. Pederson, D.J. Singh, and C. Fiolhais, *Phys. Rev.* ***B*** **46**, 6671 (1992).

[23]. J. Heyd, G.E. Scuseria, and M. Ernzerhof, *J. Chem. Phys.* **118**, 8207 (2003).

[24]. G. Kresse and J. Furthmüller, *Phys. Rev.* ***B*** **54**,11169 (1996).

[25]. P. E. Blöchl, *Phys. Rev.* ***B*** **50**, 17953 (1994).

[26] B. Tell, J.L. Shay, and H. M. Kasper, *Phys. Rev.* ***B*** **4**, 2463 (1971).

[27]. J. Pohl and K. Albe, *J. Appl. Phys*. **108**, 023509 (2010).

[28] C. Persson, Y.J. Zhao, S. Lany, and A. Zunger, *Phys. Rev.* ***B*** **72**, 035211 (2005).

[29]. M. Kumar, H. Zhao, and C. Persson, Cation vacancies in the alloy compounds of $Cu_2ZnSn(S_{1-x}Se_x)_4$ and $CuIn(S_{1-x}Se_x)_2$, *Thin Solid Films* (2012), http://dx.doi.org/10.1016/j.tsf.2012.11.063.

[30]. S. Chen, J. H. Yang, X. G. Gong, A. Walsh, and S. H. Wei, *Phys. Rev.* **B 81**, 245204 (2010).